Sound absorption of acoustic resonators with oblique perforations

J. Carbajo (iD), S. Ghaffari Mosanenzadeh, S. Kim, and N. X. Fang

View Online   **Export Citation**   **CrossMark**

ARTICLES YOU MAY BE INTERESTED IN

Sound absorption of acoustic resonators with oblique perforations

J. Carbajo,[1,a] (iD) S. Ghaffari Mosanenzadeh,[2,b] S. Kim,[2,c] and N. X. Fang[2,d]

AFFILIATIONS

[1]Department of Physics, Systems Engineering and Signal Theory, University of Alicante, San Vicente del Raspeig 03690, Spain
[2]Department of Mechanical Engineering, Massachusetts Institute of Technology, Cambridge, Massachusetts 02139, USA

[a]Author to whom correspondence should be addressed: jesus.carbajo@ua.es
[b]mosanen@mit.edu
[c]kimseok@mit.edu
[d]nicfang@mit.edu

ABSTRACT

Low-frequency airborne noise reduction is an issue of major concern in most practical cases due to the limiting space constraints. The applicability of acoustic resonators that not only work in this frequency range but can also be tuned is of great interest in many noise control applications such as muffler devices, noise barriers, or building isolation walls. This Letter studies the acoustic behavior of perforated panel absorbers with oblique perforations. Unlike more complex devices, the proposed absorber uses a simple concept that relies on the increase in the effective length of the panel by using perforations aligned obliquely with respect to the panel surface. In doing so, a shift of the resonance frequency toward low frequencies along with an increase in the sound absorption can be achieved provided that the geometrical characteristics of the absorber are properly chosen. A simple predictive model that relies on the fluid-equivalent theory was developed to investigate the acoustic properties of these absorbers, measurements in an impedance tube over additive manufactured samples serving to confirm the previous assertions. Preliminary results show the potential of these absorbers and encourage their further development for practical purposes.

Published under license by AIP Publishing. https://doi.org/10.1063/1.5132886

Low-frequency sound absorption is still a challenge for most passive noise control applications due to the space requirements to absorb large acoustic wavelengths. In this context, emerging technologies such as additive manufacturing pose a new scenario in which this and other limitations can be overcome through a more refined design of the microstructure of the absorptive systems.[1,2] Many examples of low-frequency sound absorbers whose micro-structure was designed using these 3D printing techniques can be found in the literature,[3–6] most of which consists of an array of distributed acoustic resonators. Among these, perforated panel absorbers are still very effective resonant systems but much simpler in terms of geometrical features when compared to others. These devices typically consist of a flat rigid panel with periodically arranged perforations (usually circular holes or slits) backed by an air cavity, resulting in an acoustic resonator, with the attenuation of the acoustic waves propagating through them being produced by viscothermal losses in these holes. There exist several simple techniques for lowering the resonance frequency of perforated panel absorbers, which only require the increase in the thickness of the panel, decrease in the size of the perforations, or decrease in their open area ratio or porosity. Nevertheless, the first of these would require using thicker panels, thus increasing the space requirements and total weight of the panel, which is a drawback for lightweight applications; the second one may require sub-millimetric holes, which are usually done by laser technology, resulting in rather expensive panels; and the third one, although being a good alternative, may not be appropriate in compact-sized scenarios. Alternatively, many authors proposed innovative designs that achieve an excellent low-frequency sound absorption performance by using coiled air cavities,[7,8] extended tubes,[9,10] or hybrid resonance phenomena.[11,12] Unfortunately, there is a shortage of real applications for these solutions because they are often considered too complex for practical implementation.

In this work, a perforated panel whose perforations are aligned obliquely with respect to the normal of its surface is proposed to increase the effective thickness of the panel and thus improve the low-frequency performance of the absorber. A recent example on the fabrication of a porous material having oblique perforations can be

found in the experimental work by Liu *et al.*[13] These authors showed that an increase in the perforation angle effectively shifted the resonance frequency to lower frequencies and increased the peak sound absorption coefficient. More recently, Attenborough[14] presented formulas to predict the acoustic properties of porous media having pores inclined to the surface normal and explore their sound absorption spectra. While these works constitute an excellent reference and revealed very interesting results, there are some issues related to the workability and design profile of the panels (e.g., maximum angle, arrangement of the perforations…) that are worth investigating for the sake of their practical application. In the current research, a geometrical pattern conceived to design the panel in a straight and simple manner is proposed. Moreover, this singular design avoids the presence of dead-end pores (i.e., perforations ending at the edges of the panel), thus making the fluid flow through all the panel thickness and easing the modeling of the resonator system. Figure 1 shows the proposed design for a laterally infinite perforated panel with oblique perforations.

Several theoretical models exist to predict the acoustic properties of perforated panel absorbers, with these being mainly determined by the size of the perforations, the open area ratio, the panel thickness, and the air cavity depth.[15–17] To assess the sound absorption performance of the resonator system under study and therefore better understand its acoustic behavior, a simplified approach that relies on the fluid-equivalent theory was derived.[17] For this purpose, the system is assumed to behave as a locally reacting medium, which may be an acceptable approximation for thin perforated panels with small air cavities (i.e., small compared to the wavelength of interest). Under this statement, the panel may be replaced by a homogeneous fluid layer in the macroscopic direction of propagation (i.e., perpendicular to the surface of the perforated panel), and the acoustic impedance of the whole absorber determined is defined by

$$Z = Z_{PP} - jZ_0 \cot(k_0 D),\qquad(1)$$

where Z_{PP} is the acoustic transfer impedance of the perforated panel, Z_0 the characteristic impedance of air, k_0 the wave number in air, and D the backing air cavity depth.

Considering the perforations to be narrow tubes, the theory of acoustic wave propagation in cylindrical tubes can be used to account

FIG. 1. The perforated panel with oblique perforations proposed: (a) Schematic representation (unit cell in red), (b) frontal view of a unit cell, and (c) simplified diagram including the backing air cavity of the acoustic resonator (distance between perforations, b, thickness of the panel, d, open area ratio, ϕ, radius of the perforations, R, perforation angle, θ, and air cavity depth, D).

for both viscous and thermal effects in the panel.[18] When the length of these tubes (i.e., the thickness of the panel) is much smaller than the acoustic wavelength in the air, thermal effects can be neglected and the acoustic transfer impedance of the panel is simplified to

$$Z_{PP} = \frac{1}{\phi} j\omega\rho d,\qquad(2)$$

where d is the panel thickness, ϕ the open area ratio, ω the angular frequency, and ρ the effective density of the inner air, which can be linked to the air density ρ_0 by[17]

$$\rho = \rho_0 \alpha_\infty \left(1 + \frac{\sigma\phi}{j\omega\rho_0\alpha_\infty} G_C(s)\right),\qquad(3)$$

where α_∞ is the geometrical tortuosity and σ is the flow resistivity of the panel.

For perforations with a circular cross section, $G_C(s)$ is obtained from[19]

$$G_C(s) = -\frac{s\sqrt{-j}}{4} \frac{J_1(s\sqrt{-j})}{J_0(s\sqrt{-j})} \left(1 - \frac{2}{s\sqrt{-j}} \frac{J_1(s\sqrt{-j})}{J_0(s\sqrt{-j})}\right),\qquad(4)$$

where $s = R(\omega\rho_0/\eta)^{1/2}$, R is the radius of the perforations, η is the dynamic viscosity of air, and J_0 and J_1 are the Bessel functions of the first kind and zeroth and first order, respectively. It should be noted that it was the radius of the perforations on the panel surface that was defined, not the inner one, with the effective radius being accounted for indirectly in the model by means of an equivalent tortuosity to be defined next.

Given the finite thickness of the panel, additional corrections must be done to account for the inertial effect and viscous dissipation at the front and rear surface of the panel. For the former, an equivalent tortuosity is defined as $\alpha_\infty = 1 + 2\varepsilon_e/d$, where $\varepsilon_e = (1 - 1.13\xi - 0.09\xi^2 + 0.27\xi^3)8R/(3\pi)$ is the correction length that accounts for the effective length of the medium and the interaction between the perforations,[20] with $\xi = 2(\phi/\pi)^{1/2}$; for the latter, a surface resistance term $R_S = (\eta\rho_0\omega/2)^{1/2}$ must be added twice (inlet and outlet surfaces) in Eq. (2) (divided by ϕ to account for the whole panel). On the other hand, in the case of a panel with oblique perforations, it is also necessary to account for the angle of these perforations with respect to the direction of propagation (i.e.,: the normal of the panel surface), with the following macroscopic physical parameters being then redefined as

$$\alpha_\infty = \frac{1}{\cos^2\theta} + 2\frac{\varepsilon_e}{l},\qquad(5)$$

$$\sigma = \frac{8\eta}{\phi R^2 \cos^2\theta},\qquad(6)$$

where θ is the perforation angle and $l = d/\cos(\theta)$ is the length of the oblique perforations. Note that Eq. (5) is analogous to that defined above for straight perforations (i.e., $\theta = 0°$) but replacing 1 and d by $1/\cos^2(\theta)$ and l to account for the angle of the perforations and the effective length of the panel, respectively, whereas Eq. (6) represents the flow resistivity expression for a panel whose pores are oriented an angle θ to the normal of its surface.[19]

Once the acoustic impedance of the entire absorber system was obtained, it is straightforward to calculate its sound absorption coefficient under normal incidence from
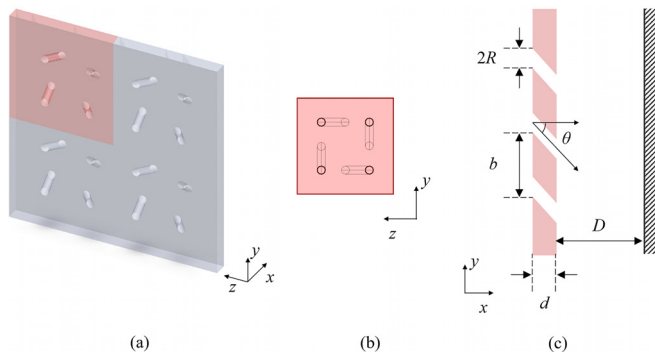
TABLE I. Geometrical parameters of the perforated panel with oblique perforations.

b (mm)	d (mm)	D (mm)	ϕ (%)	R (mm)
13.3	5	5	4	1.5

$$\alpha = 1 - \left| \frac{Z - Z_0}{Z + Z_0} \right|^2. \qquad (7)$$

Thereby, the above expression serves to predict the sound absorption behavior of a perforated panel absorber with either straight ($\theta = 0$) or oblique ($\theta \neq 0$) perforations. As an example, let us consider the perforated panel absorber with oblique perforations whose geometrical characteristics are summarized in Table I, the perforation angle values ranging from 0 to $\theta_{max} = atan(b/d)$, and $b = R(\pi/\phi)^{1/2}$ is the distance between inlet perforations. Again, it must be noted that under normal incidence conditions, it is the distance between perforations over the surface of the panel that must be considered to account for the hole interaction effects.[21] In doing so, the maximum angle to be analyzed is set so that the outlet of the perforations is constrained to the area delimited by the four inlet perforations of the unit cell depicted in Fig. 1(b). According to the proposed geometrical pattern, maximum perforation angle θ_{max} is also constrained by the distance between inlet perforations, with the values close to 90° being hardly achievable in practice. In fact, for such cases, the locally reacting assumption may not be strictly valid, with other modeling procedures being probably more appropriate. In Fig. 2, the influence of the angle of perforations on the sound absorption coefficient of the absorber under study is shown.

The results clearly demonstrate that a significant improvement of sound absorption performance of the perforated panel absorber can be achieved by using oblique perforations. Given that the path of acoustic waves through the panel is lengthened as the angle of the perforations increases, so does the effective thickness of the panel. Accordingly, resonance frequency of the absorber gradually shifts from 1830 Hz to
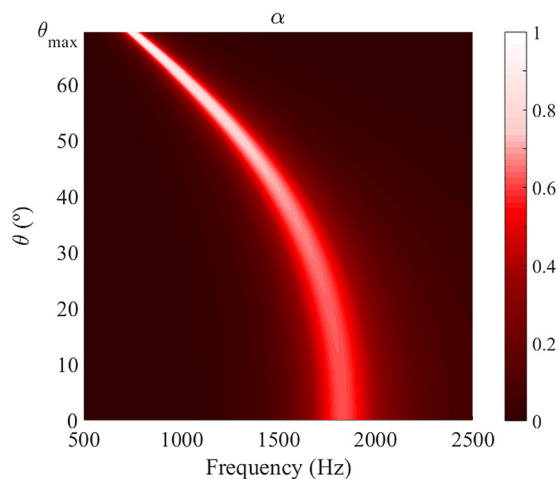
FIG. 2. Theoretical sound absorption coefficient spectra as a function of the perforation angle θ for the perforated panel whose geometrical characteristics are listed in Table I ($\theta_{max} = atan(b/d) = 69°$).

lower frequencies well below 800 Hz, resulting in the sound absorption coefficient reaching peak values higher than 0.8 at angles above 55°. In this regard, from Eq. (6), it can be deduced that the higher the perforation angle, the higher the flow resistivity value, and consequently, the energy loss occurs inside the panel due to viscous dissipation mechanisms. In brief, theoretical predictions showed that by choosing the appropriate geometrical parameters of the perforations, not only the resonance frequency of the absorber can be lowered but also its absorption amplitude is increased.

For verification purposes, a three-dimensional numerical model was implemented using the Acoustics module of the finite element software COMSOL Multi-physics® and the sound absorption results are compared with those from the proposed approach. Briefly, an impedance tube is connected to the air-cavity backed unit cell depicted in Fig. 1(b) and the sound absorption coefficient determined following the procedure described in the standard ASTM E1050.[22] Both the impedance tube and the air cavity domains were modeled as air, whereas the perforations were modeled as a fluid equivalent whose acoustic properties were retrieved from the model worked out by Zwikker and Kosten,[18] with the remaining boundaries being considered acoustically rigid. All domains were discretized using quadratic tetrahedral elements with a maximum size of 10 mm (more than ten elements for the smallest analyzed wavelength). A plane wave boundary condition was imposed at the opposite side of the acoustic resonator, with the sound absorption coefficient under normal incidence being thus evaluated from the pressure field data computed for each frequency in the numerical simulation.

To extend the analysis to panels with different geometrical features, the radius of the perforations, the open area ratio, and the panel thickness were modified while maintaining the other parameters constant. The reference values chosen for the calculations are summarized in Table I, with the angle of the perforations being set to $\theta = 40°$ for all the analyzed cases. Figure 3 shows the absorption curves for the different configurations studied.

The results show that the analytical curves are in fairly good agreement with the finite element simulations for most of the studied cases. As expected, it can be seen that reducing the radius of the perforations mainly affects the amplitude of the absorption peak for the analyzed configurations [Fig. 3(a)], whereas lower open area ratios or thicker panels produce a shift of the resonance peak to lower frequencies [Figs. 3(b) and 3(c)]. It should be noted that the surface resistance term was not included in the analytical calculations because these are not considered in the numerical model.

In order to further validate the proposed analytical model, prediction results were compared with impedance tube measurements over samples manufactured using Projection micro-stereolithography (PμSL) printing technology.[23,24] Unlike the fabrication methods commonly used to perforate panels, such as mechanical or laser drilling techniques, the PμSL technique avoids the need for angle support blocks or sophisticated positioning systems to make the oblique perforations. Moreover, geometry of the perforations can be engineered with a great accuracy using this technique, besides overcoming limitations on the slope of the overhang, which is common in other additive manufacturing processes such as Fused Deposition Modeling (FDM).[25] Experiments were therefore intended both to verify the theoretical findings and to assess the suitability of using PμSL technology for accurate fabrication of oblique perforations.
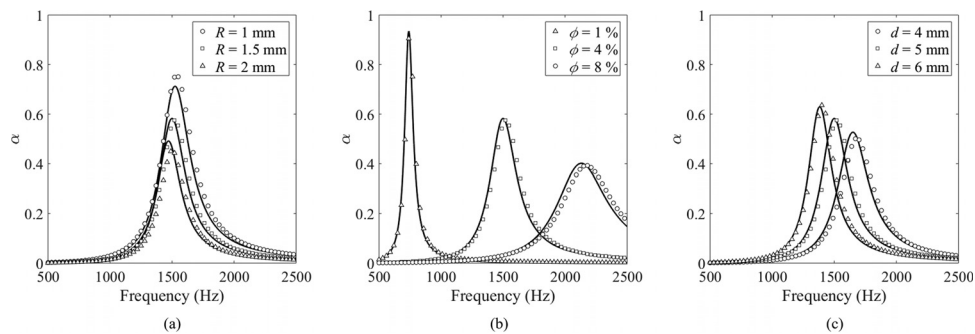
FIG. 3. Influence on the sound absorption coefficient of an acoustic resonator with oblique perforations ($\theta = 40°$) and the geometrical characteristics listed in Table I of modifying: (a) the radius of the perforations; (b) the open area ratio; and (c) the thickness of the panel. Solid line: Proposed model; markers: finite element model.

The Ember 3D printer from Autodesk was used to prepare different circular samples, with the manufacturing accuracy being 50–100 micrometers on the y- and z-axes and 10–50 micrometers on the x-axis. Only the results for three different samples will be shown, with their corresponding perforation angle values being 0°, 40°, and 60°. All these samples had the geometrical characteristics listed in Table I. The impedance tube BSWA SW470 (30 mm inner diameter) was used to determine the sound absorption coefficient of these samples following the transfer function method described in the standard ASTM E1050–12.[21] The measurement system is composed of the data acquisition card MC3522, two ¼ inch microphones MPA416, a power amplifier PA50, and the software VA-LAB2 provided by BSWA that supports the measurement and calculation of sound absorption of a material using the transfer matrix method. Figure 4 shows some pictures of the prepared samples and the corresponding sound absorption coefficient obtained both theoretically and experimentally.

It is shown that the experimental results follow the trends predicted by the simplified model. A frequency shift of 730 Hz was achieved for the sample having a perforation angle of $\theta = 60°$ when compared to the sample with straight perforations ($\theta = 0°$), with the peak absorption

value increasing up to 0.89. Discrepancies on the model predictions may be due to manufacturing accuracy (e.g., actual size of the perforations in the prepared samples show deviations of ± 0.1 mm), which is a common issue in the microstructure-based modeling of 3D-printed porous media.[26,27] It should also be noted that the arrangement of the perforations on the front surface of the panel differs from that on the rear surface [see Fig. 1(b)]. All the same, the simplified model herein proposed may serve for preliminary design purposes, and an implementation of the full linearized Navier–Stokes equations using numerical techniques such as the Finite Element Method[28] or the Boundary Element Method[29] is necessary otherwise.

Once the predictions in terms of the sound absorption coefficient showed the potential of these systems, let us now further explore the advantages of using panels with oblique perforations instead of straight ones. In the wake of the above results, a reduction in the air cavity depth in the absorber with oblique perforations is expected to still maintain a resonant frequency similar to that of the straight case. As a result, a significant reduction in the total depth of the absorber can be achieved in addition to a sound absorption enhancement. Figure 5 shows a comparison of the sound absorption coefficient of a perforated panel absorber whose geometrical characteristics are listed in Table I for the cases of straight perforations ($\theta = 0°$) with an air cavity depth of $D = 15$ mm and oblique perforations ($\theta = 60°$) with an air cavity depth of $D = 5$ mm.

The results show that the panel with oblique perforations yields almost the same resonance frequency as the panel with straight ones, while a reduction in the total depth of the absorber to half its size is achieved. Moreover, the peak absorption value is noticeably higher than that obtained for the panel with straight perforations, thus improving the sound absorption performance of these devices. In short, experimental results confirmed the previous assertions and again showed a good agreement when compared to the predictions of the simplified model.

In this work, a preliminary insight into the sound absorption potential of perforated panel absorbers with oblique perforations was given. A simple model that relies on the fluid-equivalent theory was developed to investigate the acoustic behavior of such devices. Theoretical predictions showed that a remarkable increase in the sound absorption along with a frequency shift toward low frequencies can be achieved by appropriately choosing the geometrical parameters of the panel. To verify these findings, different samples were prepared using the PµSL technique and tested using an impedance tube setup.
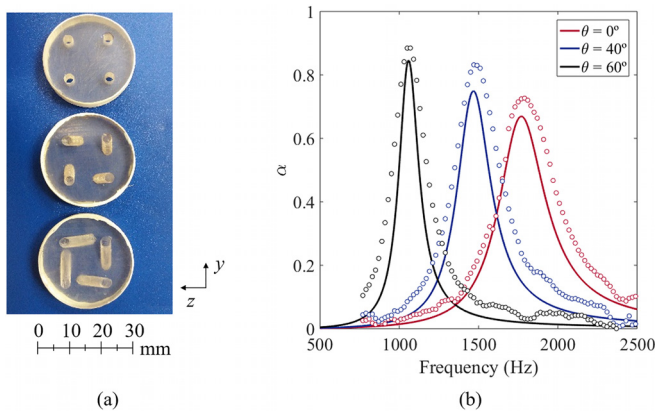

FIG. 4. (a) Picture of the 3D printed samples with oblique perforations (top: $\theta = 0°$, center: $\theta = 40°$, and bottom: $\theta = 60°$). (b) Comparison of the theoretical (continuous line) and measured (circles) sound absorption coefficient spectra for different perforation angles θ. The geometrical characteristics of the samples are summarized in Table I.
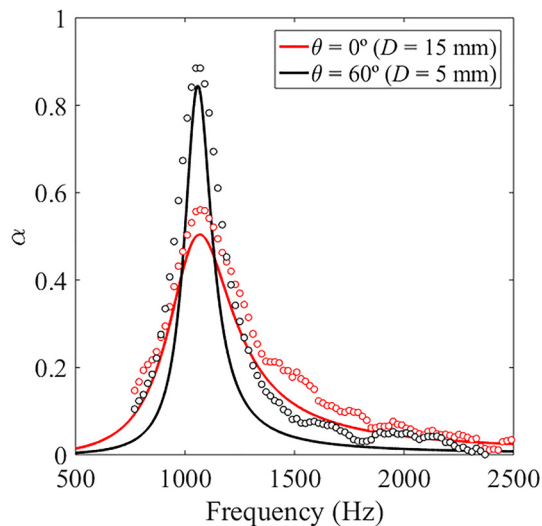
FIG. 5. Comparison of the theoretical (continuous line) and measured (circles) sound absorption coefficient spectra for two different cases: straight perforations ($\theta = 0°$) with an air cavity depth of $D = 15$ mm and oblique perforations ($\theta = 60°$) with an air cavity depth of $D = 5$ mm. The geometrical characteristics of the samples are listed in Table I.

Experimental results showed the sound absorption improvement resulting from employing oblique perforations instead of straight ones, with the model predictions showing a good agreement when compared to the measurement data. In summary, even though the acoustic effectiveness of these systems may be to some extent linked to the accuracy of the additive manufacturing process, the sound absorption and tuning capabilities encourage their practical application, while these manufacturing technologies spread out. Besides, these resonators not only yield an improved sound absorption performance when compared to conventional perforated panels but can also be conceived for such applications in which aesthetical or visual protective features are also needed.

REFERENCES

[1] F. Setaki, M. Tenpierik, M. Turrin, and A. van Timmeren, Build. Environ. **72**, 188–200 (2014).

[2] E. R. Fotsing, A. Dubourg, A. Ross, and J. Mardjono, Appl. Acoust. **148**, 322–331 (2019).

[3] N. Jiménez, W. Huang, V. Romero-García, V. Pagneux, and J.-P. Groby, Appl. Phys. Lett. **109**, 121902 (2016).

[4] M. Yang, S. Chen, C. Fu, and P. Sheng, Mater. Horiz. **4**, 673–680 (2017).

[5] T. Dupont, P. Leclaire, R. Panneton, and O. Umnova, Appl. Acoust. **136**, 86–93 (2018).

[6] H. Chang, L. Liu, and X. Hu, AIP Adv. **8**, 045115 (2018).

[7] Y. Li and B. M. Assouar, Appl. Phys. Lett. **108**, 063502 (2016).

[8] F. Wu, Y. Xiao, D. Yu, H. Zhao, Y. Wang, and J. Wen, Appl. Phys. Lett. **114**, 151901 (2019).

[9] D. Li, D. Chang, and B. Liu, Appl. Acoust. **102**, 126–132 (2016).

[10] S. Huang, X. Fang, X. Wang, B. Assouar, Q. Cheng, and Y. Li, J. Acoust. Soc. Am. **145**, 254–262 (2019).

[11] Y. Tang, F. Li, F. Xin, and T. J. Lu, Mater. Des. **134**, 502–512 (2017).

[12] H. Ryoo and W. Jeon, Appl. Phys. Lett. **113**, 121903 (2018).

[13] Z. Liu, J. Zhan, M. Fard, and J. L. Davy, Mater. Lett. **181**, 296–299 (2016).

[14] K. Attenborough, Appl. Acoust. **130**, 188–194 (2018).

[15] D. Y. Maa, Noise Control Eng. J. **29**(3), 77–84 (1987).

[16] L. L. Beranek and I. L. Ver, *Noise and Vibration Control Engineering: Principles and Applications* (John Wiley & Sons, 2006).

[17] N. Atalla and F. Sgard, J. Sound Vib. **303**, 195–208 (2007).

[18] C. Zwikker and C. W. Kosten, *Sound Absorbing Materials* (Elsevier, 1949).

[19] J. F. Allard and N. Atalla, *Propagation of Sound in Porous Media: Modelling Sound Absorbing Materials* (John Wiley & Sons, 2009).

[20] L. Jaouen and F. X. Bécot, J. Acoust. Soc. Am. **129**(3), 1400–1406 (2011).

[21] R. Tayong, Appl. Acoust. **74**(2), 1492–1498 (2013).

[22] ASTM Standard E1050-12, *Standard Test Method for Impedance and Absorption of Acoustic Materials Using a Tube, Two Microphones and a Digital Frequency Analysis System* (American Society for Testing and Materials, 2012).

[23] C. Sun, N. Fang, D. M. Wu, and X. Zhang, Sens. Actuators, A **121**(1), 113–120 (2005).

[24] X. Zheng, H. Lee, T. H. Weisgraber, M. Shusteff, J. DeOtte, E. B. Duoss, J. D. Kuntz, M. M. Biener, Q. Ge, J. A. Jackson, S. O. Kucheyev, N. X. Fang, and C. M. Spadaccini, Science **344**(6190), 1373–1377 (2014).

[25] M. Vaezi, H. Seitz, and S. Yang, Int. J. Adv. Manuf. Technol. **67**, 1721–1754 (2013).

[26] P. V. Pisarev, A. N. Anoshkin, and K. A. Maksimova, AIP Conf. Proc. **2027**, 040079 (2018).

[27] T. G. Zieliński and M. Červenka, in *Proceedings of Internoise 2019* (Spanish Acoustical Society/International Institute of Noise Control Engineering, 2019), p. 1695.

[28] J. Carbajo, J. Ramis, L. Godinho, P. Amado-Mendes, and J. Alba, Appl. Acoust. **90**, 1–8 (2015).

[29] V. Cutanda, P. Risby, J. J. Jensen, P. M. Juhl, and J. Sánchez-Dehesa, J. Comput. Acoust **25**(4), 1750006 (2017).